USING THE OUTSKIRTS OF GALAXY CLUSTERS TO MEASURE THEIR MASS ACCRETION RATE

C. De Boni[1,2,3]★, A. L. Serra[4], A. Diaferio[2,3], C. Giocoli[5,6,7,8], M. Baldi[6,7,8]

[1]Institut d'Astrophysique Spatiale, CNRS (UMR8617) Université Paris-Sud 11, Bât. 121, F-91405 Orsay, France; [2]Dipartimento di Fisica, Università di Torino, via P. Giuria 1, I-10125 Torino, Italy; [3]INFN, Sezione di Torino, via P. Giuria 1, I-10125 Torino, Italy; [4]Dipartimento di Fisica, Università di Milano, via Celoria 16, I-1033 Milan, Italy; [5]Aix Marseille Université, CNRS, LAM (Laboratoire d'Astrophysique de Marseille) UMR 7326, F-13388 Marseille, France; [6]Dipartimento di Fisica e Astronomia, Alma Mater Studiorum Università di Bologna, viale Berti Pichat 6/2, I-40127 Bologna, Italy; [7]INAF, Osservatorio Astronomico di Bologna, via Ranzani 1, I-40127 Bologna, Italy; [8]INFN, Sezione di Bologna, viale Berti Pichat 6/2, I-40127 Bologna, Italy; ★E-mail: cristiano.deboni@ias.u-psud.fr

THE MASS ACCRETION HISTORY

We are interested in investigating the growth of structures at nonlinear scales of galaxy clusters from an observational perspective, which is still relatively poorly explored.

In the current model of structure formation, where dark matter halos form from the aggregation of smaller halos, the mass accretion of dark matter halos is a stochastic process whose average behavior can be predicted with *N*-body simulations and semi-analytical models. This process is generally investigated with the identification of the merger trees of dark matter halos, enabling the study of the mass accretion history (MAH) and its derivative with respect to cosmic time, the mass accretion rate (MAR), as a function of redshift z.

Here we explore the possibility of estimating the MAR of galaxy clusters by measuring the mass of a spherical shell surrounding the cluster. This approach provides a method to estimate the MAR that depends on the cluster mass profile at radii larger than the virial radius.

We need to verify that our simple approach is capable of correctly estimating the actual MAR, so we compare the MAR estimated with our recipe with the MAR of dark matter halos derived from their halo merger trees obtained in an *N*-body simulation.

For this work we use the CoDECS suite of numerical simulations (www.marcobaldi.it/CoDECS).

We select halos with median $M_{200} = 10^{14}$ and 10^{15} $M_\odot$ h^{-1} at $z = 0$. The low-mass bin contains 2000 objects at z = 0, while the high-mass bin is limited to 50 objects. For each halo in the two mass bins and for each progenitor at higher redshift, we evaluate the mass profile and the profile of the radial velocity v_{rad} up to $10R_{200}$.

For each halo at $z = 0$ in the two mass bins we build the MAH at R_{200} and at $2R_{200}$ (Figure 1). $2R_{200}$ roughly correspond to the outermost radius reached by the accreted material in its first orbit around the cluster center, the so-called splashback radius. This radius is not affected by the evolution of the critical density of the universe, unlike the usual R_{200}. By adopting R_{200}, part of the mass evolution with redshift simply is a consequence of the evolution of the critical density; this effect is generally called pseudo-evolution. This pseudo-evolution substantially disappears if we adopt $M(<2R_{200})$.

Fig. 1: MAH at $2R_{200}$ for the 10^{14} $M_\odot$ h^{-1} (left panel) and 10^{15} $M_\odot$ h^{-1} (right panel) mass bins.

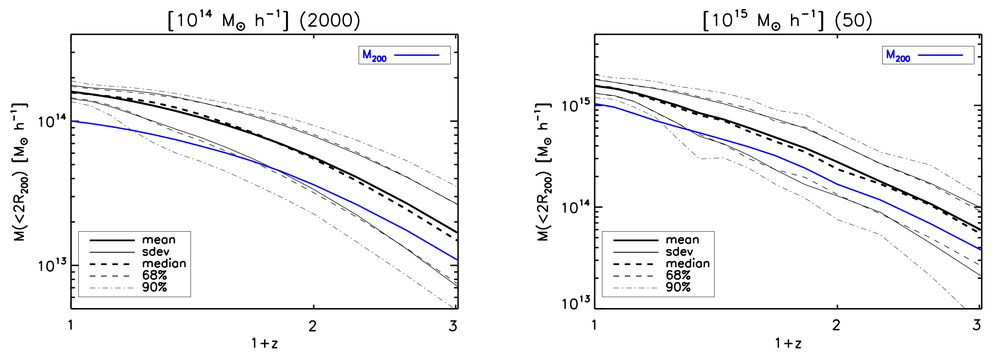

THE SPHERICAL INFALL MODEL

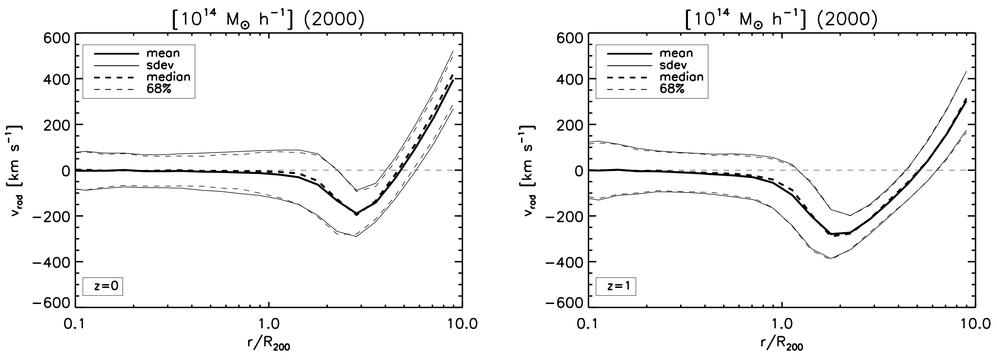

Fig. 2: Radial velocity profile for clusters in the 10^{14} $M_\odot$ h^{-1} mass bin at $z = 0$ (left panel) and $z = 1$ (right panel).

With the radial velocity profile we can identify three regions: an internal region with $v_{rad} \approx 0$, where matter is orbiting around the center of the cluster; an infall region, where v_{rad} becomes negative and indicates an actual infall of matter toward the center of the cluster; and a Hubble region at very large radii, where v_{rad} becomes positive and the Hubble flow dominates.

Broadly speaking, the infall radius R_{inf}, i.e., the radius where the minimum of v_{rad} occurs, is between $2R_{200}$ and $3R_{200}$, independently of mass and redshift.

We show the radial velocity profile in the 10^{14} $M_\odot$ h^{-1} bin at different redshifts in Figure 2.

Our spherical infall prescription assumes a shell of matter falling onto the enclosed halo.

We aim to quantify the mass accretion rate (MAR) as the ratio between the mass of a spherical shell of thickness $\delta_s R_i$ and the time it takes to fall onto the halo.

The thickness δ_s depends on the initial radius of the cluster R_i, on the infall time t_{inf}, and on the initial infall velocity v_i.

Given that $M(<2R_{200})$ is not affected by pseudo-evolution, we use $R_i = 2R_{200}$ as the radius at which we consider the infall to happen in our spherical infall prescription and $v_i \approx v_{rad}(R_{inf})$.

For the infall time, which is the last parameter of the model, we choose $t_{inf} = 10^9$ yr, similar to the dynamical time, simply defined as $t_{dyn} \approx R/\sigma$, for the clusters of our analysis. In fact, for the 10^{14}-10^{15} $M_\odot$ h^{-1} clusters at $z = 0$ we consider here, $R \approx 1$ Mpc and $\sigma \approx 1000$ km s^{-1}, and $t_{dyn} \approx 1$ Gyr. For the progenitors of these clusters at higher redshifts, which have masses at most a factor 10 smaller, the velocity dispersion σ is $10^{1/2} \approx 3$ times smaller, and the virial radius R is smaller by roughly a similar factor. Therefore, t_{dyn} remains basically constant and equal to 1 Gyr.

This value is also suggested by the redshift-independent ≈ 1 Gyr time step of the snapshots of the simulation used to estimate the MAR from the merger trees; if t_{inf} departs too much from the snapshot time interval, the comparison of our estimated MAR's with the MAR's extracted from the merger trees would be inappropriate.

Once R_i, v_i and t_{inf} are specified, the model is completely determined. For each halo in the two mass bins and for each progenitor at higher redshift, we evaluate the thickness δ_s of the infalling shell and its mass.

We show the evolution with redshift of the shell thickness δ_s in Figure 3. The shell thickness increases with increasing redshift, and the intrinsic scatter of the distribution also enlarges. This fact reflects the individual evolution of $M(<2R_{200})$, as shown in Figure 1. The solid blue line in Figure 3 marks the value $\delta_s = 0.5$ for which the external radius of the shell is equal to $3R_{200}$, close to the cluster turnaround radius. This value of δ_s is reached between redshift 1 and 1.5, depending on the mass of the cluster.

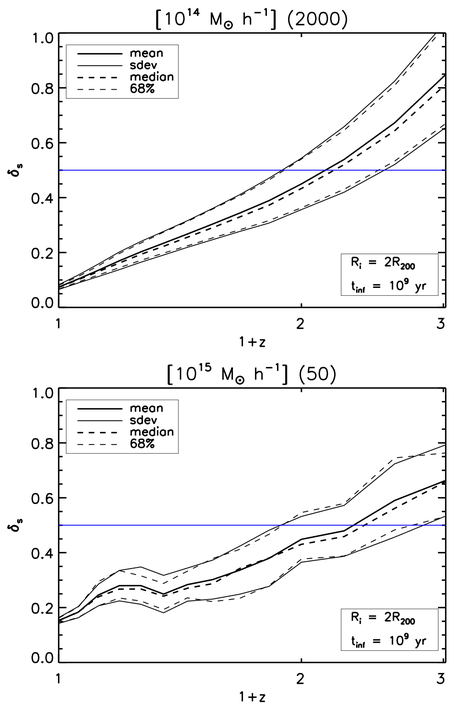

Fig. 3: Redshift evolution of the shell thickness δ_s for the 10^{14} $M_\odot$ h^{-1} (top panel) and the 10^{15} $M_\odot$ h^{-1} (bottom panel).

RESULTS

De Boni et al. 2016, ApJ, 818, 188

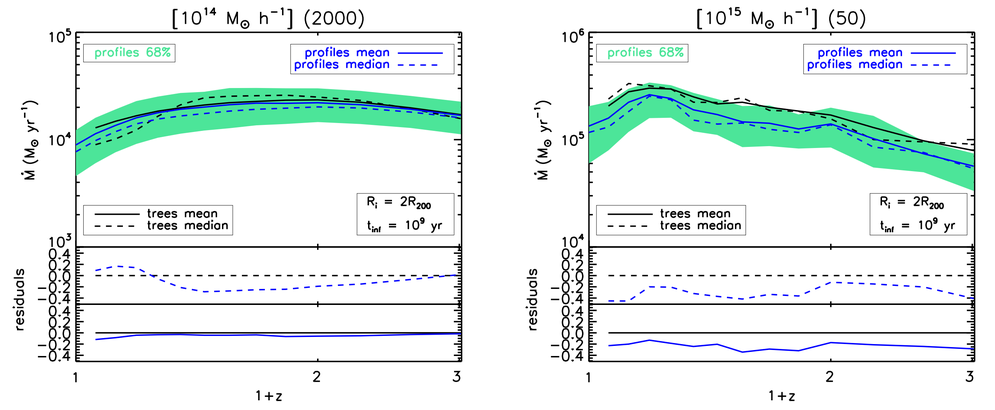

Fig. 4: Results of our spherical infall model for the 10^{14} $M_\odot$ h^{-1} (left panel) and 10^{15} $M_\odot$ h^{-1} (right panel) mass bins and comparison with the MAR from merger trees.

Figure 4 shows the MAR of all the clusters in the two mass bins estimated with our spherical infall prescription. It also shows the MAR derived from the merger trees of the halos.

The mean and median results from the merger trees lie within the region defined by the 68% range of the distribution of the MAR's obtained with our spherical infall prescription for both mass bins.

For the 10^{15} $M_\odot$ h^{-1} bin, the mean and median values of our estimate are ≈ 40% smaller than the average MAR values from the merger trees. This systematic underestimate might be due to a statistical fluctuation because the sample only contains 50 clusters compared with the 2000 clusters of the less massive bin.

In contrast, for the 10^{14} $M_\odot$ h^{-1} mass bin, the mean and median MAR from our prescription recover the merger tree results within 20% in the redshift range $z = [0,2]$.

Clearly Figure 4 only compares the average MAR obtained from the merger trees of individual halos with the average MAR provided by our spherical infall technique. Our recipe was not conceived to completely capture all the features of the MAR derived by the complex merging process of individual halos. Nevertheless, the average of the MAR of individual halos still is satisfactorily estimated by our recipe.

Our results are relevant because they show that our simple spherical infall prescription can in principle provide a method to estimate the average MAR of galaxy clusters from redshift surveys.

Figure 5 shows the distribution of the ratio between the MAR estimated with our recipe and the MAR derived from the merger tree for each individual halo of the 10^{14} $M_\odot$ h^{-1} mass bin at two different redshifts.

The distribution has a tail towards large values. Remarkably, the median value of this ratio is close to the ratio between the average MAR from our model and the MAR from the merger trees (red line). The mean clearly is larger because of the tail of high values. The 68% ranges from 0.2 to 2.2. This results confirms that with our approach we can measure the mean MAR but not the MAR of the individual clusters, which is affected by lack of spherical symmetry and large variations of the infall velocity.

Figures 1 and 2 show the intrinsic halo-by-halo scatter both in radial velocity and mass. Our choice to use the same v_{inf} for all clusters in a given mass bin at a given redshift implies that we neglect the scatter that originates the spread of the distribution shown in Figure 5. However, this choice keeps the model relatively simple and applicable to real clusters.

It is worth saying that the impact of the large-value tail is reduced if we take the ratio of the averages of the MAR of each individual halo estimated with our prescription and with the merger trees, rather than the average of the ratio. The ratio of averages is shown with the red line in Figure 5 and it corresponds to the result shown in Figure 4.

The remarkable and encouraging result of our analysis is that the agreement shown in Figures 4 and 5 is obtained without requiring any input information from the merger trees.

A fundamental step to asses the feasibility of our approach is to apply the caustic technique to realistic mock redshift surveys of galaxy clusters extracted from the same *N*-body simulations and quantify the accuracy of the estimated MAR.

Similarly the analysis of the dependence of the method parameters and its results on the cosmological model and on the theory of gravity remain to be investigated.

The final goal is to apply our spherical infall recipe to the clusters in the CIRS and HeCS catalogs whose outer mass profiles have already been measured with the caustic technique.

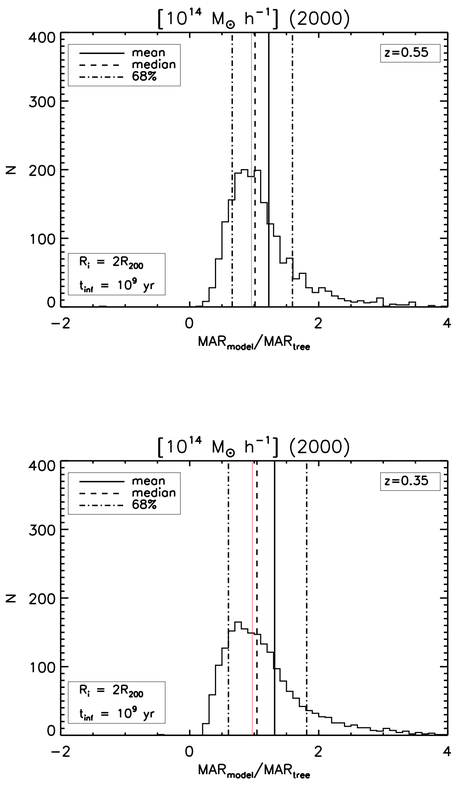

Fig. 5: Histogram of the halo-by-halo ratio between the MAR from our spherical infall model and the MAR from the merger trees at z = 0.35 (top panel) and z = 0.55 (bottom panel), for the 10^{14} $M_\odot$ h^{-1} mass bin.

AKNOWLEDGMENTS

We sincerely thank Fabio Fontanot for providing us with the merger trees of the H-CoDECS simulation. We thank Aaron Ludlow, Margherita Ghezzi, Giulio Falcioni, and Andrea Vittino for useful discussions. C. D. B., A. L. S., and A. D. acknowledge partial support from the grant Progetti di Ateneo/CSP TO_Call2_2012_0011 ``Marco Polo" of the University of Torino, the INFN grant InDark, and the grant PRIN_2012 ``Fisica Astroparticellare Teorica" of the Italian Ministry of University and Research. A. L. S. also acknowledges the support of Dipartimento di Fisica, University of Torino, where most of this project was carried out. C. G.'s research is part of the project GLENCO, funded under the European Seventh Framework Programme, Ideas, Grant Agreement n. 259349. C. G. also thanks CNES for financial support. M. B. is supported by the Marie Curie Intra-European Fellowship ``SIDUN" within the 7th Framework Programme of the European Commission. This work was partially supported by grants from Région Ile-de-France. Soundtrack: Justine Brisy.